AD

TECHNICAL REPORT ARCCB-TR-92017

CHARACTERIZATION OF RESIDUAL STRESSES IN AN ECCENTRIC SWAGE AUTOFRETTAGED THICK-WALLED STEEL CYLINDER

S.L. LEE
G.P. O'HARA
V. OLMSTEAD
G. CAPSIMALIS

APRIL 1992

US ARMY ARMAMENT RESEARCH,
DEVELOPMENT AND ENGINEERING CENTER
CLOSE COMBAT ARMAMENTS CENTER
BENÉT LABORATORIES
WATERVLIET, N.Y. 12189-4050

DISCLAIMER

The findings in this report are not to be construed as an official Department of the Army position unless so designated by other authorized documents.

The use of trade name(s) and/or manufacturer(s) does not constitute an official indorsement or approval.

DESTRUCTION NOTICE

For classified documents, follow the procedures in DoD 5200.22-M, Industrial Security Manual, Section II-19 or DoD 5200.1-R, Information Security Program Regulation, Chapter IX.

For unclassified, limited documents, destroy by any method that will prevent disclosure of contents or reconstruction of the document.

For unclassified, unlimited documents, destroy when the report is no longer needed. Do not return it to the originator.

REPORT DOCUMENTATION PAGE

Form Approved
OMB No. 0704-0188

1. AGENCY USE ONLY (Leave blank)	2. REPORT DATE	3. REPORT TYPE AND DATES COVERED
	April	Final

4. TITLE AND SUBTITLE

CHARACTERIZATION OF RESIDUAL STRESSES IN AN ECCENTRIC SWAGE AUTOFRETTAGED THICK-WALLED STEEL CYLINDER

5. FUNDING NUMBERS

AMCMS No. 6126.24.H180.0
PRON No. 1A1TZ1FBNMFP

6. AUTHOR(S)

S.L. Lee, G.P. O'Hara, V. Olmstead, G. Capsimalis

7. PERFORMING ORGANIZATION NAME(S) AND ADDRESS(ES)

U.S. Army ARDEC
Benet Laboratories, SMCAR-CCB-TL
Watervliet, NY 12189-4050

8. PERFORMING ORGANIZATION REPORT NUMBER

ARCCB-TR-92017

9. SPONSORING/MONITORING AGENCY NAME(S) AND ADDRESS(ES)

U.S. Army ARDEC
Close Combat Armaments Center
Picatinny Arsenal, NJ 07806-5000

10. SPONSORING/MONITORING AGENCY REPORT NUMBER

11. SUPPLEMENTARY NOTES

Presented at the ASM International Topical Conference on the Practical Applications of Residual Stress Technology, Indianapolis, IN, 15-17 May 1992
Published in the Proceedings of the Conference

12a. DISTRIBUTION/AVAILABILITY STATEMENT

Approved for public release; distribution unlimited

12b. DISTRIBUTION CODE

13. ABSTRACT *(Maximum 200 words)*

In the swage autofrettage process, partial autofrettage was achieved by driving an oversized mandrel through the cylinders to cause plastic deformation. In this work, we made experimental and theoretical investigations of residual stresses in a swaged asymmetric thick-walled cylinder with small wall variations. Hoop and radial residual stress distributions, as well as angular hoop stress variations at the inside and outside diameter of the cylinder, were determined by using a single-exposure position-sensitive scintillation x-ray diffraction detection system. Our experimental results were in good agreement with the residual stress distributions predicted from Tresca's hydraulic autofrettage model. Deviations of hoop residual stress at the bore may be attributed to Bauschinger's effect. Finite element analysis using ABAQUS code on a Convex supercomputer was used to model the swage autofrettage process. Small angular residual stress variations were predicted due to the eccentricity of the cylinder. The finite element model predictions of residual stress distribution were in general agreement with experimental results except near the bore. Preliminary results of an alternative finite element method showed a reduced compressive hoop stress near the bore, similar to the results obtained by assuming Bauschinger's effect.

14. SUBJECT TERMS	15. NUMBER OF PAGES
Residual Stress, Finite Element Analysis, Pressure Vessel, Reverse Yielding, Eccentric Cylinder, X-Ray Diffraction, Swage Autofrettage, Bauschinger's Effect, ABAQUS Code	25
	16. PRICE CODE

17. SECURITY CLASSIFICATION OF REPORT	18. SECURITY CLASSIFICATION OF THIS PAGE	19. SECURITY CLASSIFICATION OF ABSTRACT	20. LIMITATION OF ABSTRACT
UNCLASSIFIED	UNCLASSIFIED	UNCLASSIFIED	UL

TABLE OF CONTENTS

LIST OF ILLUSTRATIONS

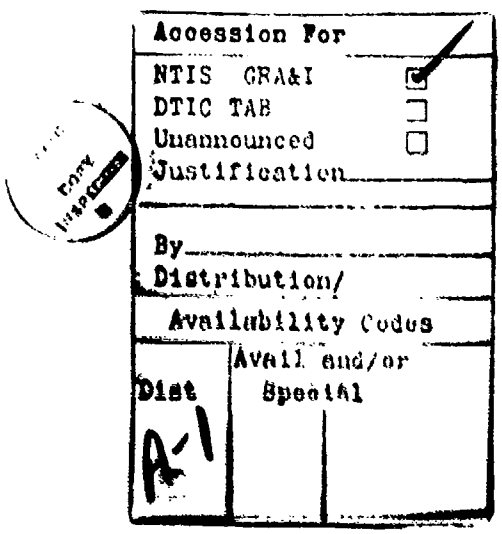

INTRODUCTION

The autofrettage process involves the application of radial forces at the bore of a cylinder with sufficient magnitude to cause permanent bore expansion. Mechanical swage autofrettage eliminates the ultrahigh pressures required in the conventional hydraulic method to produce the same radial forces (refs 1,2). As a result, the residual stress distribution increases the elastic strength of the cylinder, retards the growth of fatigue cracks at the cylinder bore, and improves the roundness and straightness of the cylinder. Work on mandrel geometry design requiring minimum load has been reported (ref 3). However, limited work has been done in the evaluation of the mandrel design and the swage process by residual stress measurements. Furthermore, in the manufacturing process, an asymmetric cylinder resulting from the boring process is generally rejected without knowledge of the effects on residual stresses. In the present investigation, residual stress measurements were made using the x-ray diffraction (XRD) method on a single-exposure position-sensitive scintillation detection (PSSD) system. Our experimental results were compared with (1) predictions made by assuming Tresca's yield criterion, and (2) a finite element model that treats the swage autofrettage process as a ram, mandrel, and cylinder three-body problem.

SPECIMEN PREPARATION

Figure 1 is a schematic diagram of the swaging process including the carbide tool. Figure 2 is a cross-sectional view of the eccentric tube. The cylinder under investigation had an outside radius of 15.69 cm (6.19 in.) and an inside bore radius of 5.69 cm (2.24 in.), giving an outside diameter/inside diameter (OD/ID) ratio of 2.75. Radially forged cylinders underwent a number of finishing operations during the manufacturing process. The inner bore of the

forged cylinder was honed. Subsequently, the entire cylinder was subjected to plastic deformation by pushing a tungsten carbide tool through the bore. The interference between the ID of the cylinder and the load diameter of the carbide tool, which is 2.5 percent, determines the amount of plastic deformation. The inside radius of the cylinder was 5.69 cm (2.24 in.) before autofrettage and 5.77 cm (2.27 in.) after autofrettage. The bore was rough-machined, and a substantial portion of the tube was removed to eliminate 'end effects' during the swage process. The wall variation due to the boring process was found at this stage, and the cylinder was rejected. The after-processing wall thickness was 9.93 cm (3.91 in.) at 0 degree (thickest) and 9.68 cm (3.81 in.) at 180 degrees (thinnest). This gave a maximum wall variation of 2.54 mm (0.1 in.) and an eccentricity of 1.27 mm (0.05 in.).

A 3.81-cm (1.50-in.) thick ring was cut from the cylinder and was machine- and hand-polished. Electropolishing of the entire cross section of the ring was done by the Chrome Plating Facility, Watervliet Arsenal, Watervliet, NY. The polishing solution was a mixture of 50 percent sulfuric acid and 50 percent phosphoric acid heated to 130°F; the anode was a tank lead piece; the voltage was 7 to 8 V; the current was 2 amp/in.^{2}; and the cathode-to-anode distance was 10 to 15 cm (4 to 6 in.). No external agitation device was used. It took 45 minutes to remove 5 mils from the surface of the ring. Surface material was removed so that sanding, machining, and oxidation effects would not influence the residual stress measurements.

EXPERIMENTAL METHOD

A D-1000-A Denver X-Ray Instruments Model stress analyzer design was used based on a Ruud-Barrett PSSD system. The instrumentation and calibration procedures for the analyzer are described in References 4 and 5. The system utilizes

a chromium target tube, and the K-α reflects from the 211 plane of the body-centered-cubic (BCC) steel at 2θ = 156.41 degrees.

Although local multiple-exposure ($\sin^2\psi$) software has been developed, the present measurements exclusively used the single-exposure method. This was due to the large number of measurements required to cover the 1-foot diameter surface. The surface was sectioned into 32 equal parts at an 11.25-degree span each. Data acquisition was set at three iterations at 2 seconds each. The data presented were the average of three measurements at each point on the surface of the specimen. For stress distribution determination, a specimen holder with a micrometer slide was used. Angular stress variation measurements were made by manually rotating and positioning the specimen. Taking into account the dispersion in the data, the alignment error, focusing error, and effects due to surface irregularities, the stress values were expected to have an error range of ± 10 to 15 Ksi. An IBM AT computer was used for data acquisition, control, and analysis. SYMPHONY software was used for further data analyses and graphics.

X-RAY RESIDUAL STRESS MEASUREMENTS AND PREDICTIONS BASED ON TRESCA'S YIELD CRITERION

Hoop and radial residual stresses at 50 and 100 percent overstrain conditions based on Tresca's yield criterion are shown in Figure 3. Tresca's theory assumes that the thick-walled cylinder is overstrained by direct internal pressure and that an open-end condition is present (ref 6). The results were obtained by setting up a SYMPHONY spreadsheet program with varying ID, OD, and percentage overstrain parameters. Because of the different stress conditions to induce the overstrain in the swage method compared with the direct pressure

method, the actual stress distribution may differ. In Figure 4, classical theoretical stresses, including reverse yielding, are shown assuming $\alpha = 0.5$, where α is the ratio of the yield stress in compression to the yield stress in tension in a stress-strain curve for gun steels (ref 7).

The measured hoop and axial stresses versus radial distance at 0, 90, 180, and 270 degrees are shown in parallel plots in Figure 5. The 0-degree measurement position is where the ring is the thickest at 6.02 cm (2.37 in.), and the 180-degree measurement position is where the ring is the thinnest at 5.77 cm (2.27 in.). The plots show that all four curves follow the same common features as the compressive stresses observed at the bore and the tensile stresses observed at the OD. Furthermore, the Bauschinger effect is observed in all four plots, with the 180-degree plot showing the steepest reduction of compressive hoop residual stress near the bore and coupled reduction of tensile stress near the OD.

Figures 6 and 7 show hoop and axial residual stresses at 0 and 180 degrees, respectively. Hoop stresses at 90 and 270 degrees are given in Figures 8 and 9, respectively. The theoretical predictions assume 75 percent overstrain condition and are in fairly good agreement with our experimental results. The deviations in hoop stresses can be attributed to reverse yielding effects. The large ID hoop stress difference (-110 Ksi at 0 degree, -75 Ksi at 180 degrees) might justify the cylinder rejection, pending further experimental and theoretical verifications. Similar large deviations in hoop stresses in a cylinder have been reported in the literature (ref 8). Radial stresses do not quite converge to zero at the OD. It is interesting that the reverse yielding effects on hoop stress are observed in all four plots. At 180 degrees, which is the thinnest section of the cylinder, more pronounced effects exist.

Angular hoop stress variations at the ID and OD are shown in Figure 10. The measurements at the ID show a peak around 180 degrees and a smaller peak around 0 degree. The OD measurements do not show pronounced peaks. The angular stress results are in good agreement with measurements made on a Technology for Energy Corporation (TEC) stress analyzer (ref 9).

ABAQUS FINITE ELEMENT MODEL

A finite element model using ABAQUS code was run on a Convex C-220 supercomputer. Residual stress analysis in cylinders can be accomplished by three different methods: (1) the use of classic closed-form equations assuming the plane-stress end conditions and elastic-perfectly plastic material properties; (2) the finite element analysis of a cross section using improved material definition, plastic deformation at the bore during unloading, and eccentric geometry; and (3) the full modeling of the complete problem with the mandrel sliding through the tube. The third method adds many more practical details including proper mandrel geometry, moving contact, and friction at the interface, and it also requires extensive computer resources. The second method was initially chosen to evaluate the magnitude of the eccentric bore effect.

The analysis was performed using the generalized plane-strain elements to model one-half of the cross section of the tube at the time of the swage process. A total of 154 elements was defined using 7 rows in the radial direction and 22 rows in the angular direction. The eccentric geometers were produced by shifting the outer row of grid points relative to the inner row in increments of 0.10, 0.21, 0.50, and 1.0 cm (0.039, 0.078, 0.197, and 0.394 in., respectively). The load was applied by using fixed radial displacements at the inner row of nodes, which more closely approximates the action of the tungsten carbide swage mandrel than a uniform hydraulic pressure. The ABAQUS material

stress-strain curve used was almost identical to results taken from an independent experiment for steel with about the same yield strength (162 Ksi or 1116 Mpa) as the production tube. The material was defined using five linear segments which fit the data in a least squares sense.

As shown in Figures 11 and 12, the finite element model predicts little change in residual stresses due to reasonable values of eccentricity shown in decimeters. These are plots of hoop stress versus radius at the thickest (0-degree) and thinnest (180-degree) cylinder sections. It can be seen that the bore stresses are virtually the same. Farther at the outside of the tube, the eccentricity must be large to produce major effects. The hoop and radial stresses have the same features as the experimental results shown in Figures 5 through 9, except for the hoop stresses near the bore. However, the results clearly can not explain the experimental angular stress variation results shown in Figure 10. The predicted hoop and radial stresses for a symmetric cylinder using this finite element analysis are shown in Figure 13.

The differences between the measured and calculated hoop stresses near the bore have usually been attributed to the Bauschinger effect. An alternative finite element solution to the problem, using full finite element modeling of the whole cylinder as mentioned above, for a 105-mm cylinder is presented in Figure 14 (ref 10). This work was a full analysis of the swage process in a typical tube section and produced a residual hoop stress distribution much like the experimental data. This analysis was done without any reference to the Bauschinger effect and still showed a similar shape in the hoop stress distribution.

SUMMARY

The following is a summary of our experimental and theoretical investigations of the eccentric swage autofrettaged thick-walled steel cylinder:

1. Our XRD experimental results satisfactorily characterized the hoop and radial residual stress distributions of a swage autofrettaged cylinder.

2. Our experimental results in residual stress distribution were in fairly good agreement with Tresca's theoretical predictions. The deviations could be accounted for by the Bauschinger effect. Further theoretical analysis in this area will continue.

3. Our ABAQUS finite element swage autofrettage model predictions of residual stress distribution were in general agreement with our experimental values, except at the bore, where experimental hoop stresses were less compressive. Preliminary results using an alternative finite element analysis can predict the same residual stress behaviors near the bore as the Bauschinger effect.

4. Our experimental angular distributions of hoop residual stress at the ID and OD showed peaks around 0 degree (thickest) and 180 degrees (thinnest). Our finite element model predicted very small variations in hoop and radial stresses even at large eccentricities. Variations in material properties, imperfection in the electropolishing process, and unknown effects due to the manufacturing processes may be the cause.

5. Future investigations include experimental hardness determination and theoretical characterization of the cylinder using a refined finite element model.

REFERENCES

1. T. E. Davidson, C.S. Barton, A.N. Reiner, and D.P. Kendall, "A New Approach to the Autofrettage of High Strength Cylinders," Experimental Mechanics, February 1962, pp. 33-40.

2. T.E. Davidson and D.P. Kendall, "The Design of Pressure Vessels for Very High Pressure Operation," WVT-6917, Watervliet Arsenal, Watervliet, NY, May 1969.

3. P.S. Rughupathi and T. Altan, "Improvement of tne Life of Carbide Tools Used in Autofrettage-Swaging of Gun Barrels," Final Report Contract No. DAAA22-79-C-0212, Battelle Columbus Laboratories, Columbus, OH, August 1980.

4. C.O. Ruud, "Position-Sensitive Detector Improves X-Ray Powder Diffraction," Industrial Research and Development, Vol. 25, No. 1, January 1983, p. 84.

5. S.L. Lee, M. Doxbeck, and G. Capsimalis, "X-Ray Diffraction Study of Residual Stresses in Metal Matrix Composite-Jacketed Steel Cylinders Subjected to Internal Pressure," ARCCB-TR-92007, Benet Laboratories, Watervliet, NY, March 1992; also in: Nondestructive Characterization of Materials IV, (C.O. Ruud, J.F. Bussiere, and R.E. Green, eds.), Plenum Press, New York, 1991, pp. 419-427.

6. T.E. Davidson, D.P. Kendall, and A.N. Reiner, "Residual Stresses in Thick-Walled Cylinders Resulting From Mechanically-Induced Overstrain," Experimental Mechanics, November 1963, pp. 253-262.

7. S.L. Lee, "Residual Stress Analysis in an Eccentric Pre-pressurized Swage Autofrettaged Thick-Walled Cylinder," FY91 AH61 Report, U.S. Army Armament Research, Development, and Engineering Center, Picatinny Arsenal, NJ.

8. G. Clark, "Residual Stresses in Swage-Autofrettaged Thick-Walled Cylinders," Materials Research Laboratories Report MRL-R-847, Department of Defence Support, Commonwealth of Australia, 1982.

9. S.L. Lee, M. Doxbeck, and D. Snoha, "Comparison of Three Bi-Axial Stress Analyzers for Residual Stress Determination," U.S. Army ARDEC Technical Report, Benet Laboratories, Watervliet, NY, in preparation.

10. P. O'Hara, unpublished results, U.S. Army ARDEC, Benet Laboratories, Watervliet, NY.

SIMPLIFIED SCHEMATICS OF THE SWAGE PROCESS

Benét Labs

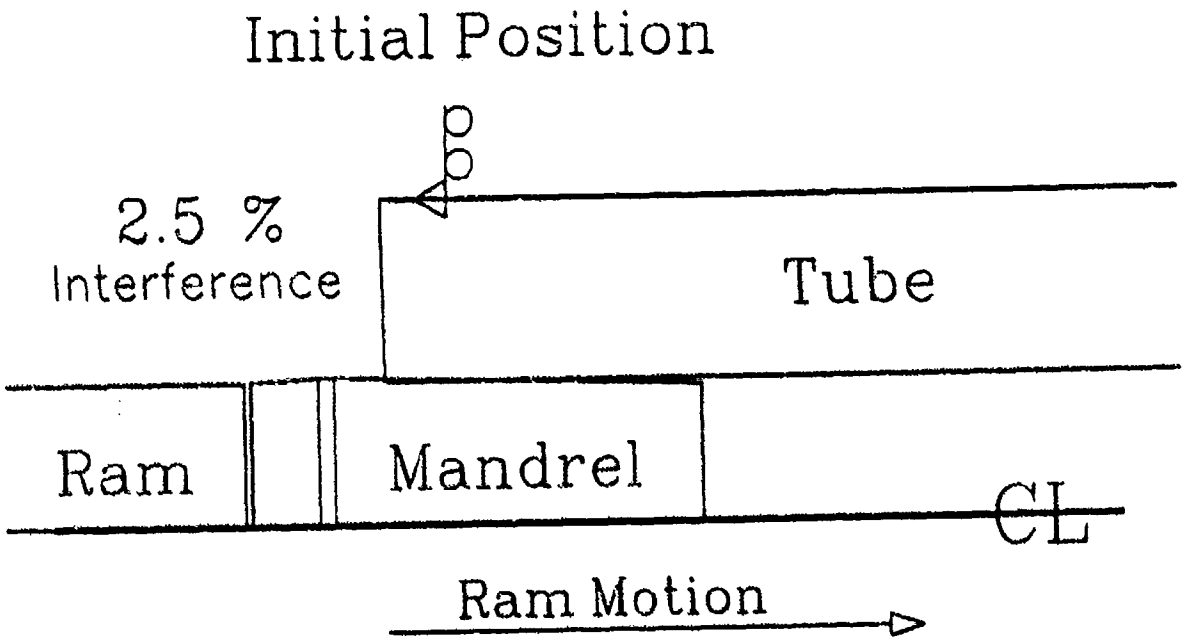

Figure 1. Partial view of ram-mandrel-cylinder swage autofrettage geometry.

GEOMETRY OF THE ECCENTRIC TUBE

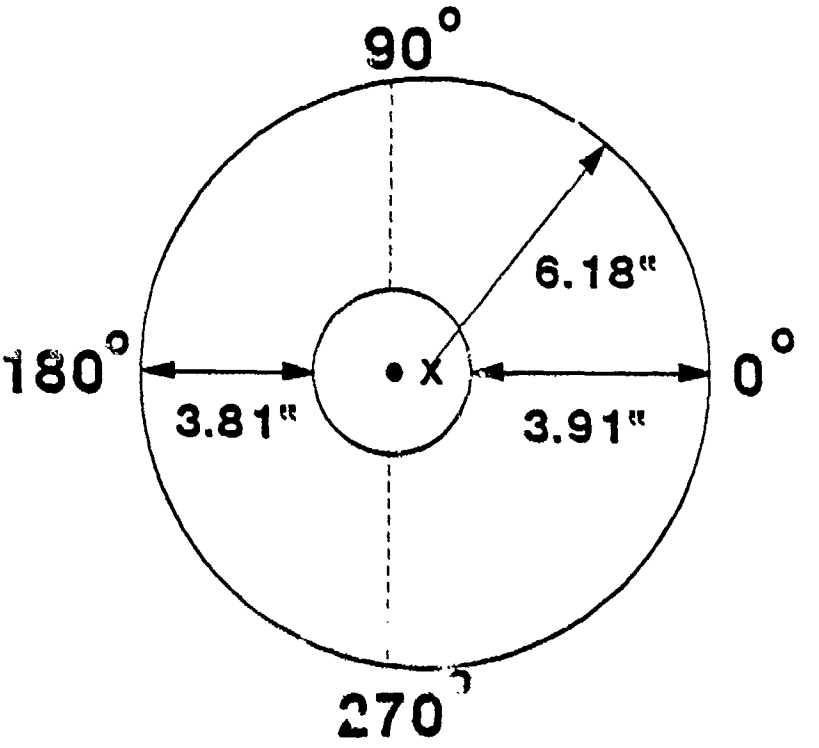

ECCENTRICITY = 0.05"

Figure 2. Geometry of the cross section of the eccentric tube.

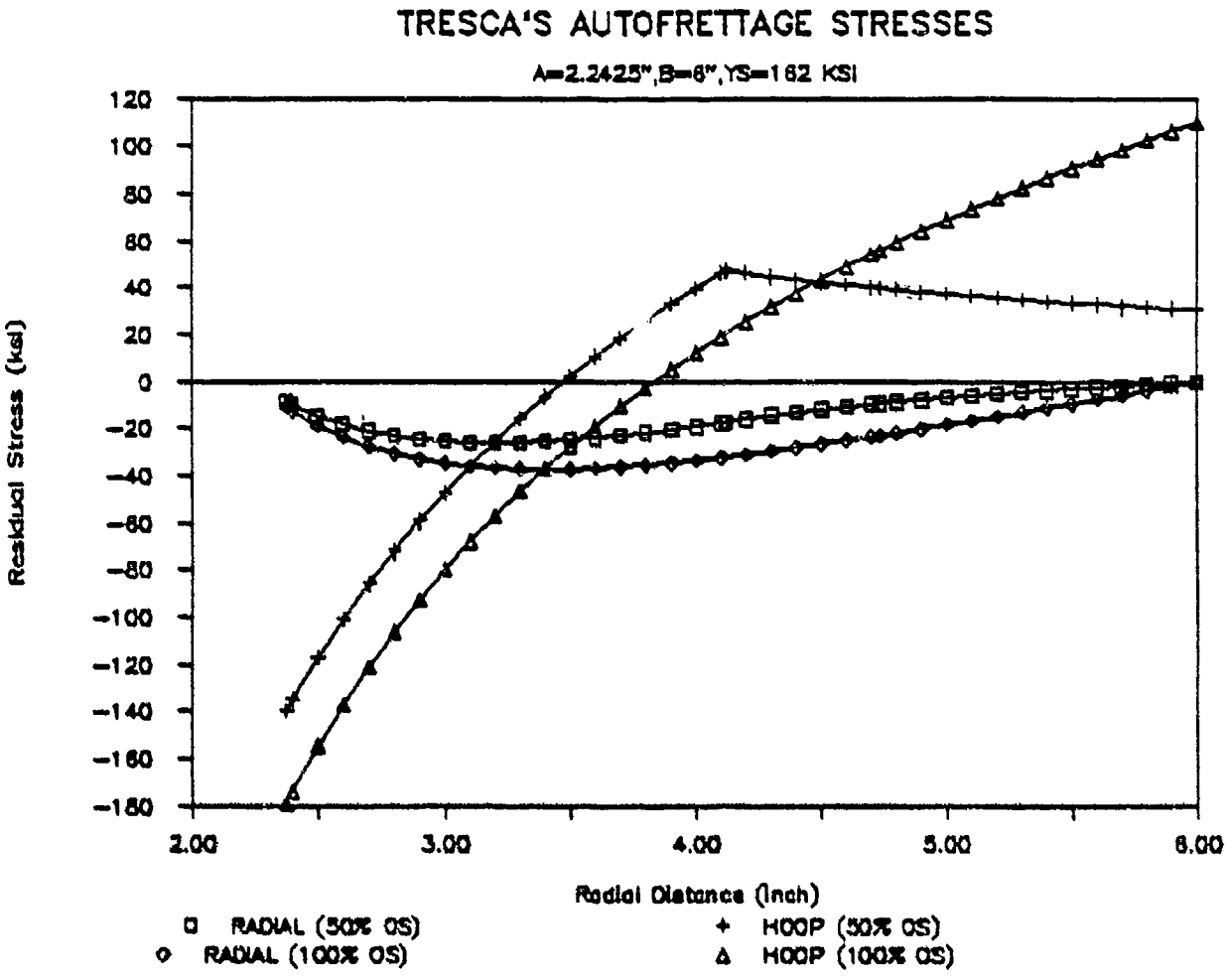

Figure 3. Theoretical hoop and radial stress distribution along the cylinder radius predicted by assuming Tresca's yield criterion.

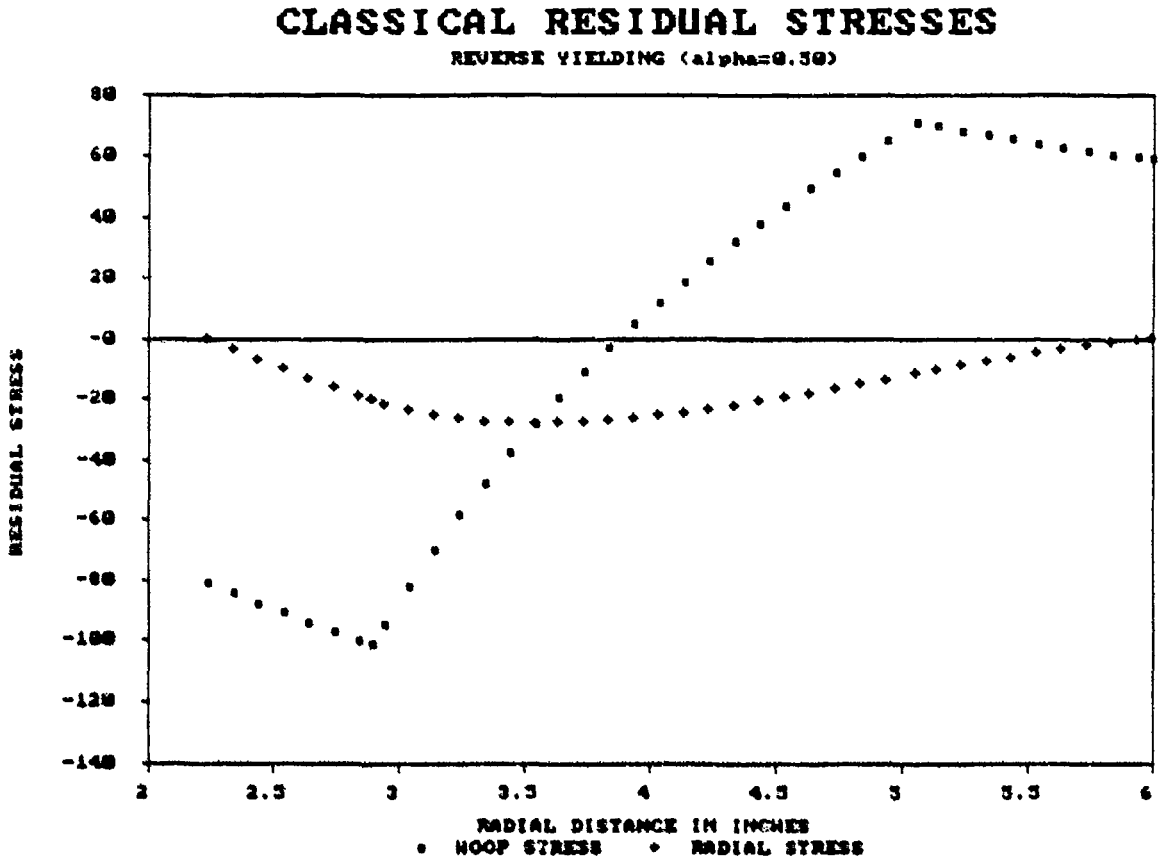

Figure 4. Theoretical stress distribution assuming Tresca's yield distribution and including reverse yielding.

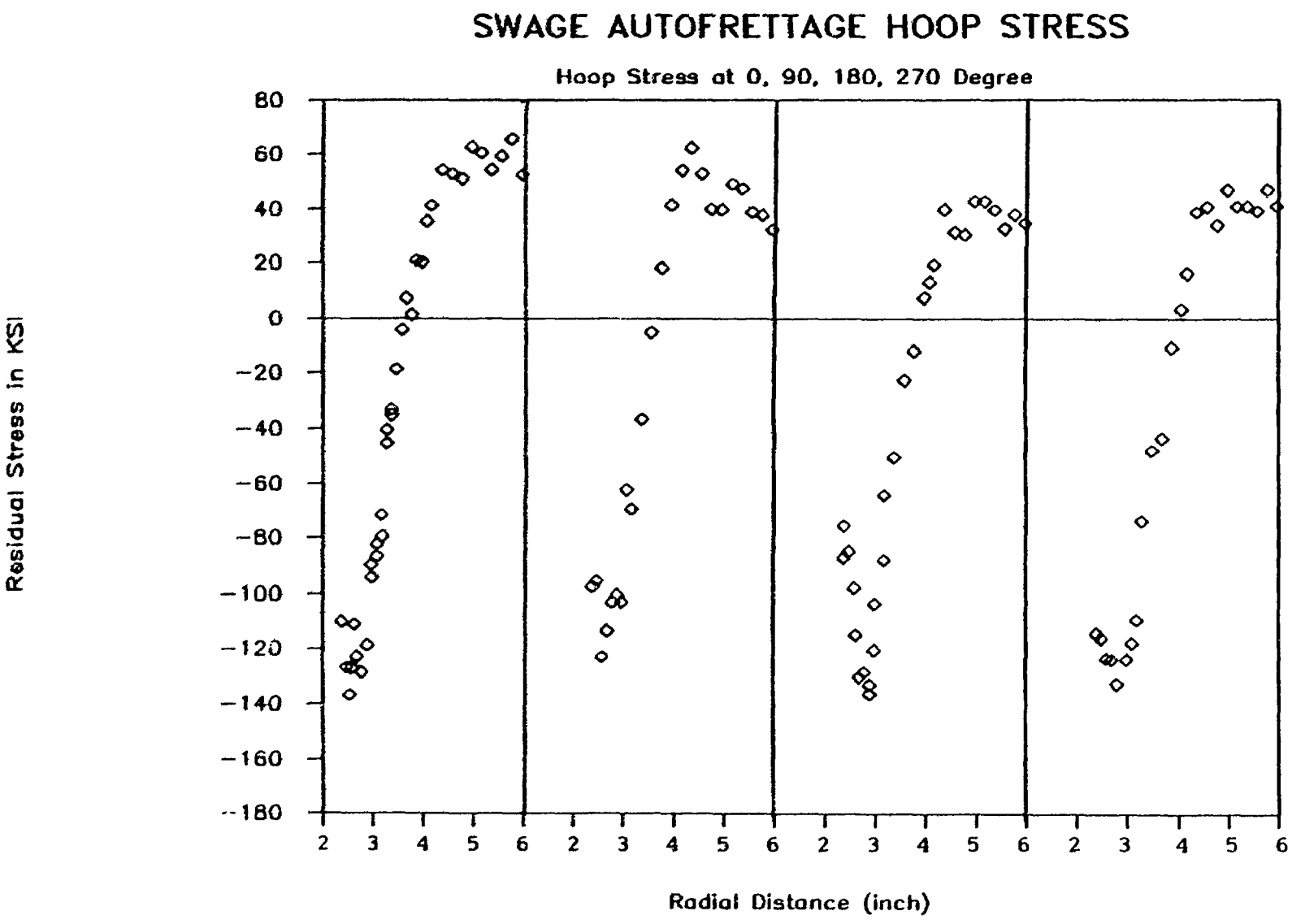

Figure 5. Hoop residual stresses along the radius at 0 (thickest section), 90, 180 (thinnest section), and 270 degrees of the M256 eccentric cylinder.

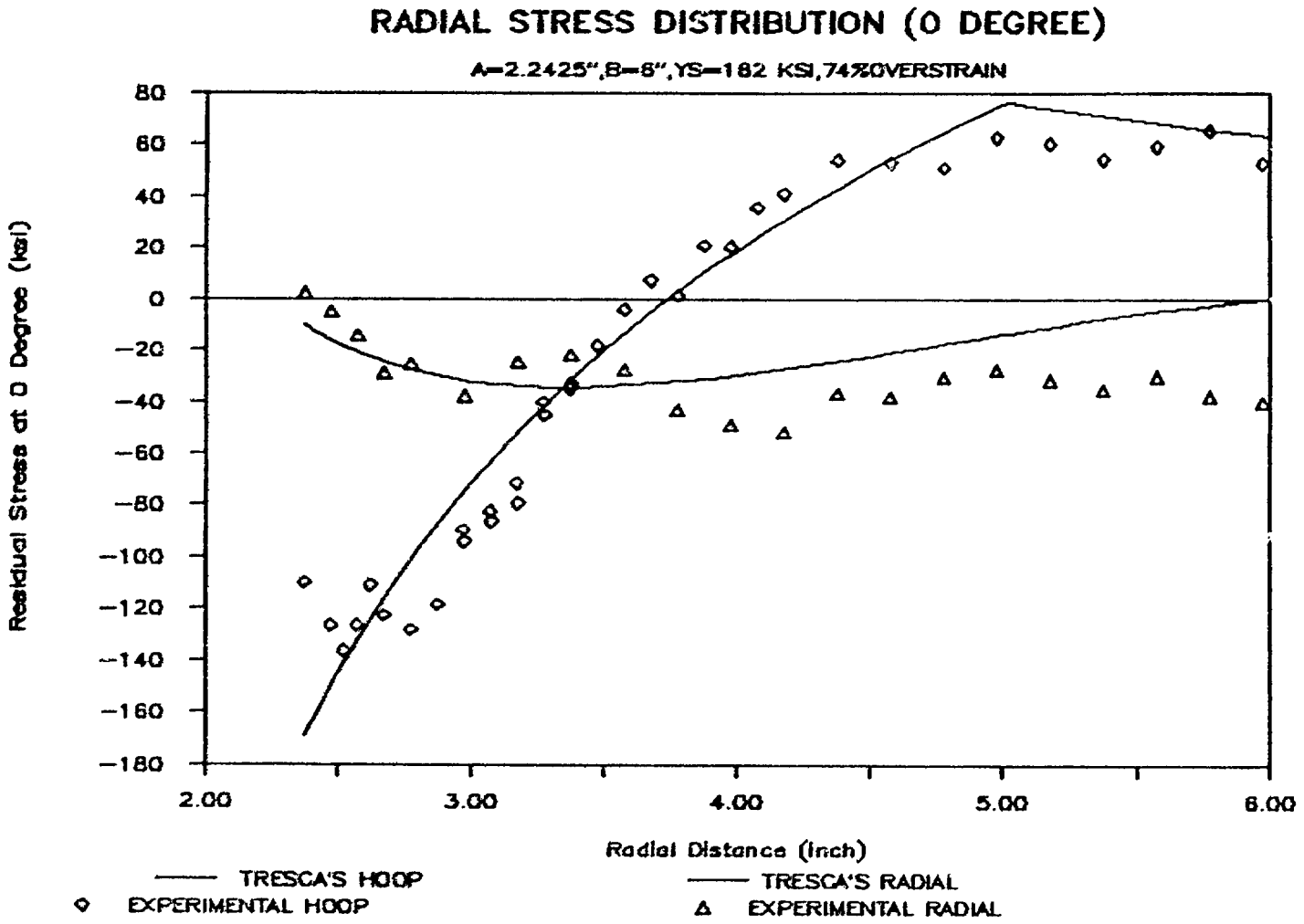

Figure 6. Hoop and radial stresses at 0 degree (thickest section).

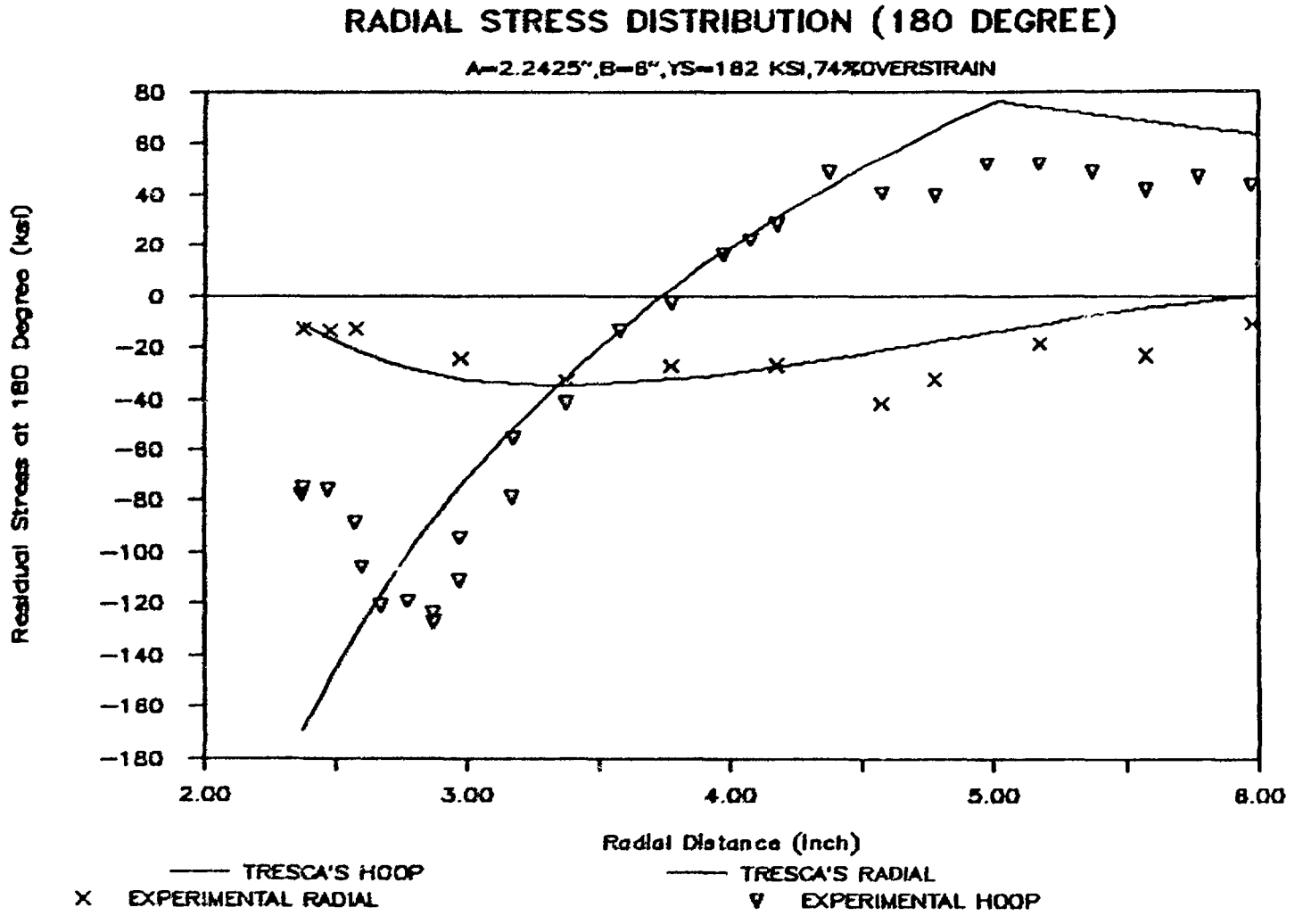

Figure 7. Hoop and radial stresses at 180 degrees (thinnest section).

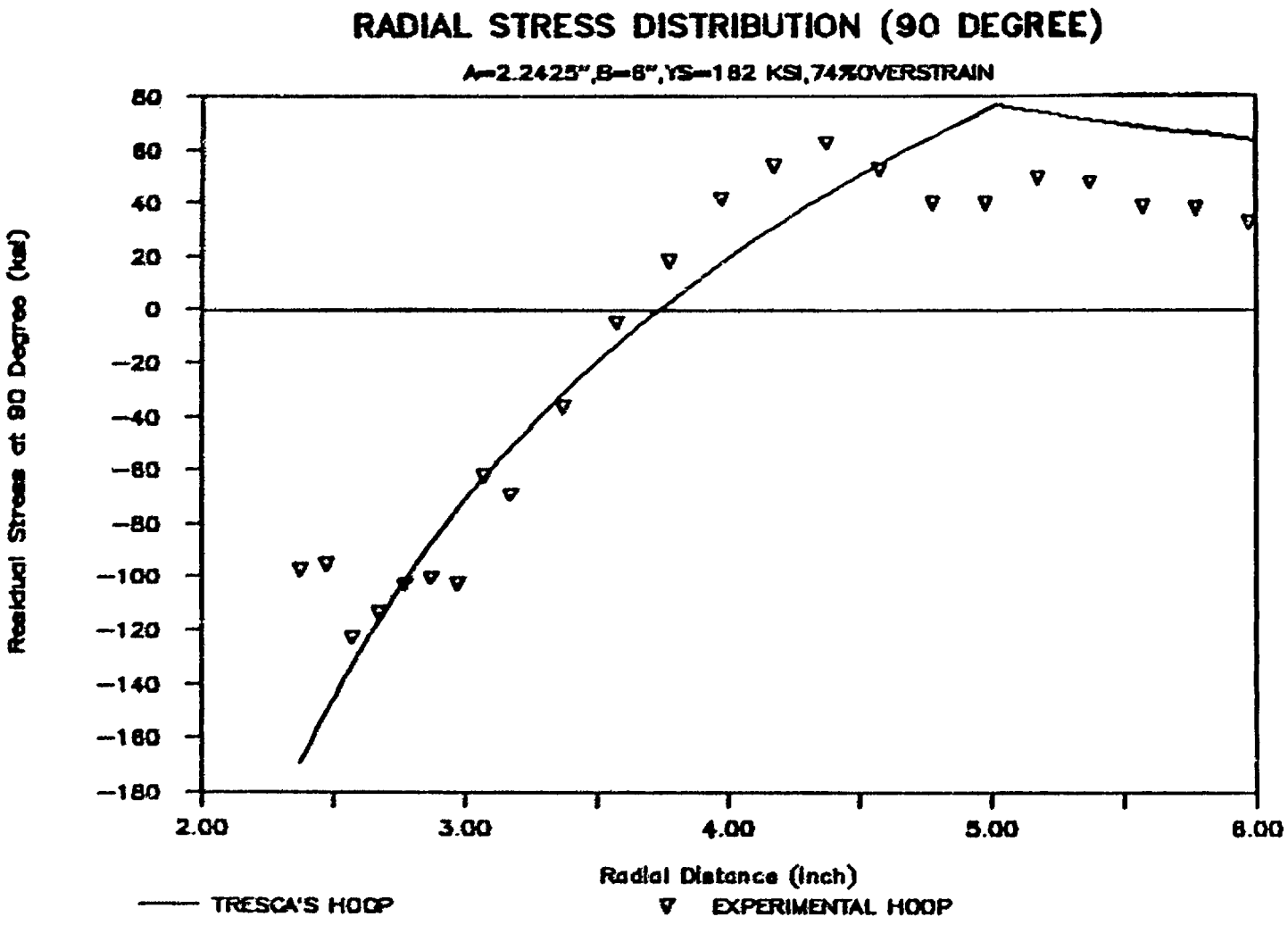

Figure 8. Hoop stress at 90 degrees.

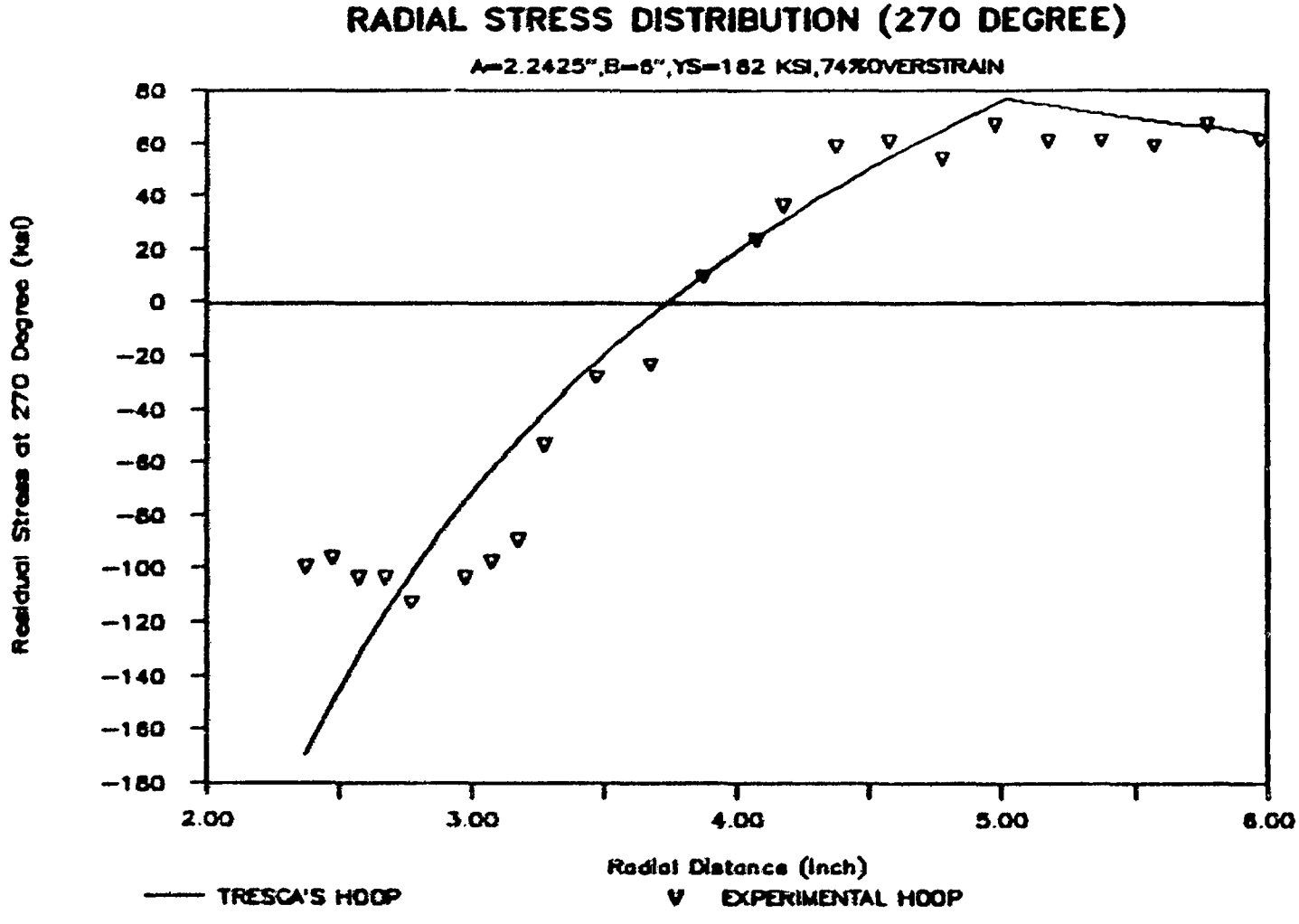

Figure 9. Hoop stress at 270 degrees.

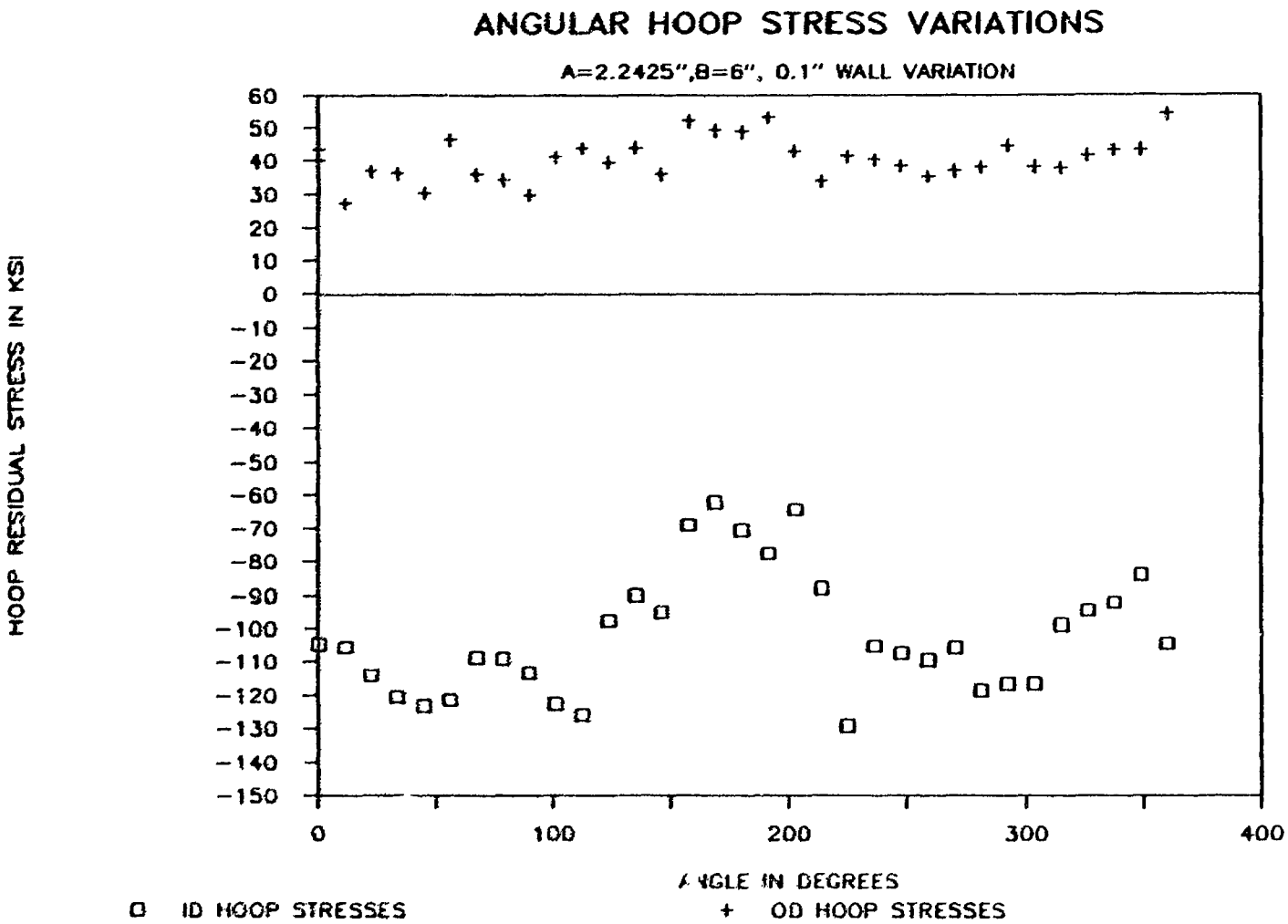

Figure 10. Angular hoop residual stresses around the cylinder.

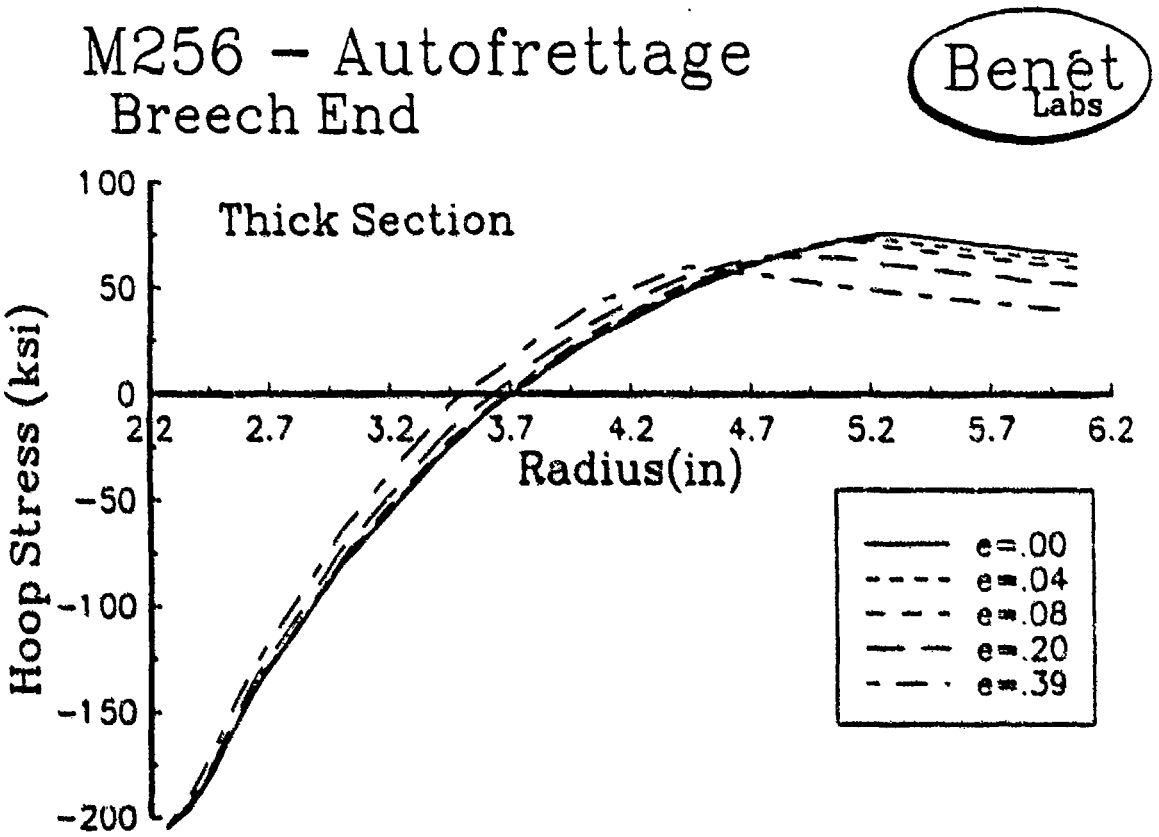

Figure 11. Finite element model hoop stress at 0 degree (thickest section) with varying eccentricity.

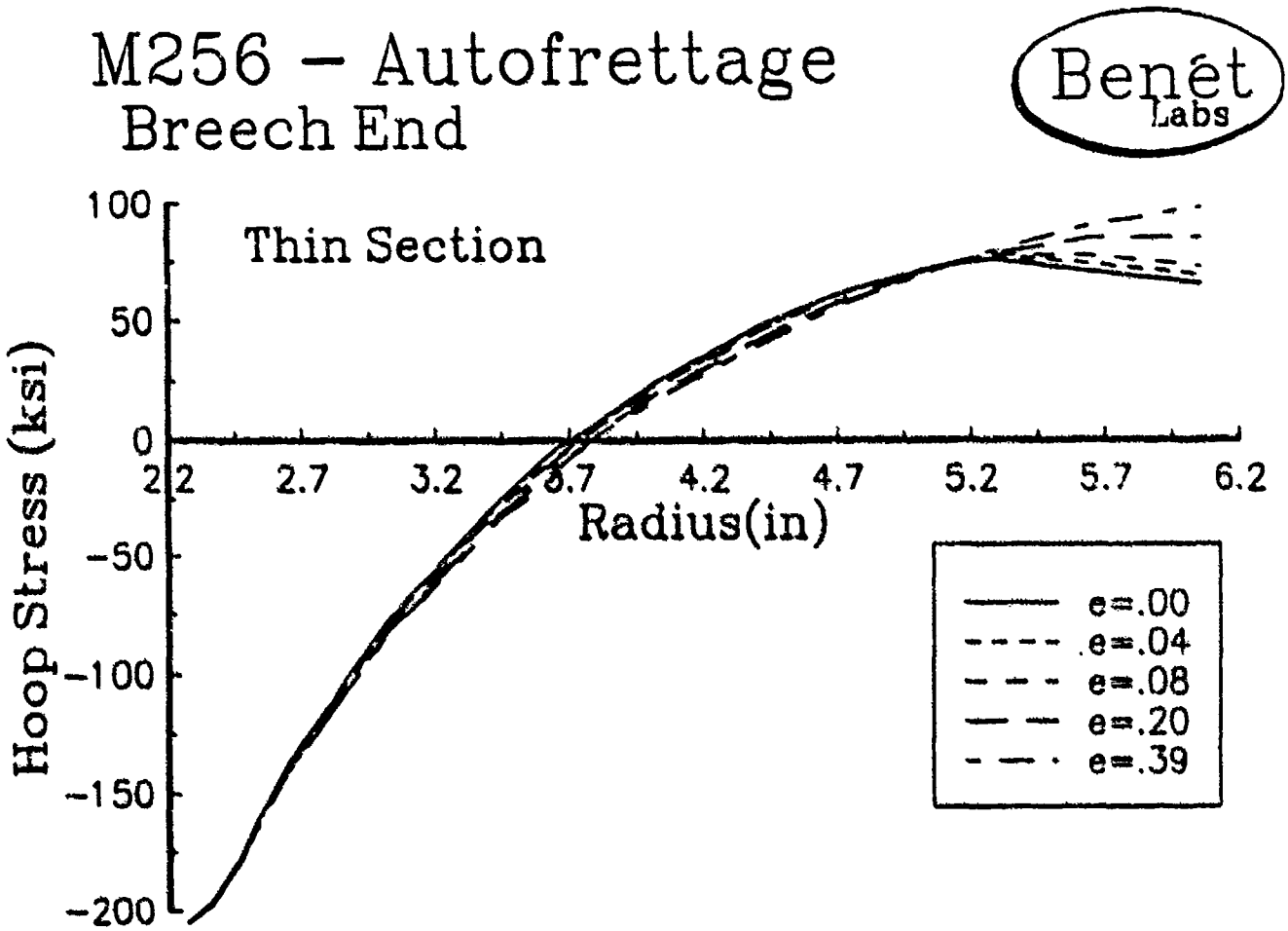

Figure 12. Finite element model hoop stress at 180 degrees (thinnest section) with varying eccentricity.

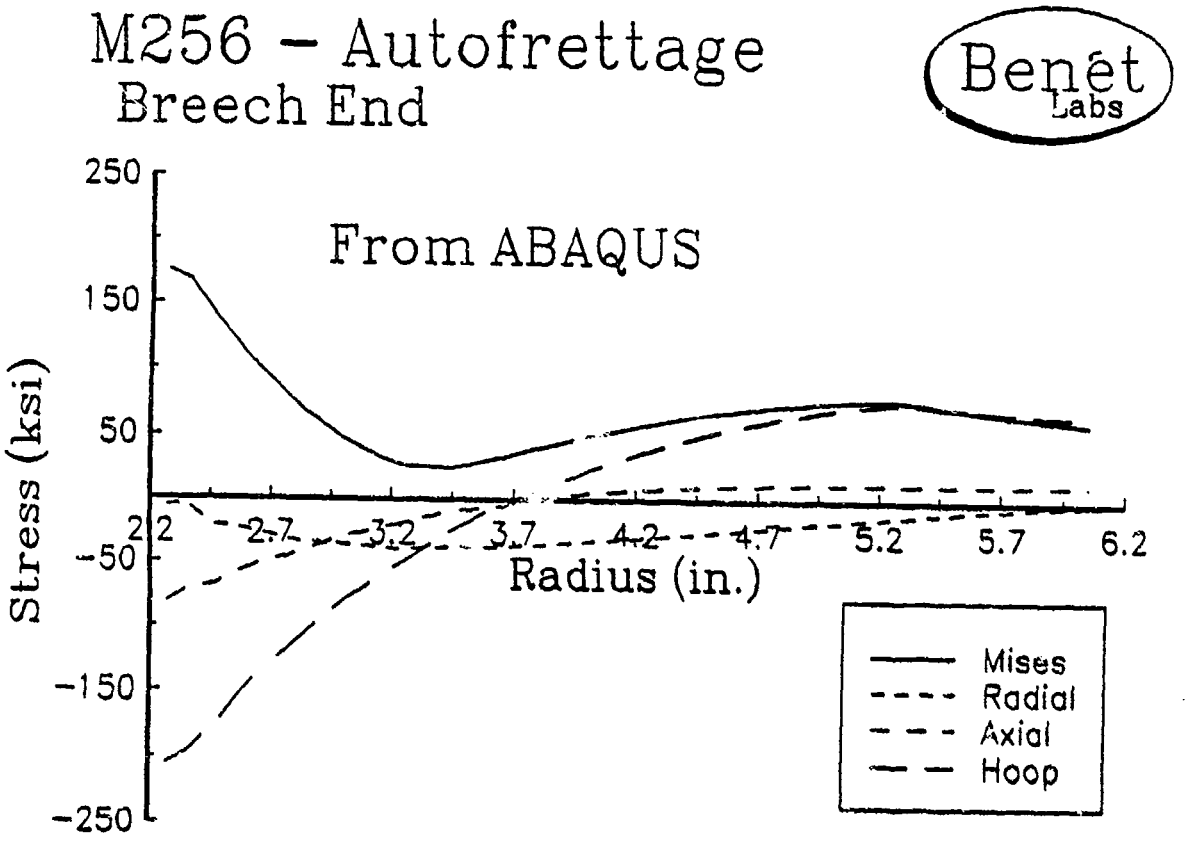

Figure 13. ABAQUS predictions of residual stresses of an M256 symmetric cylinder using the finite element method.

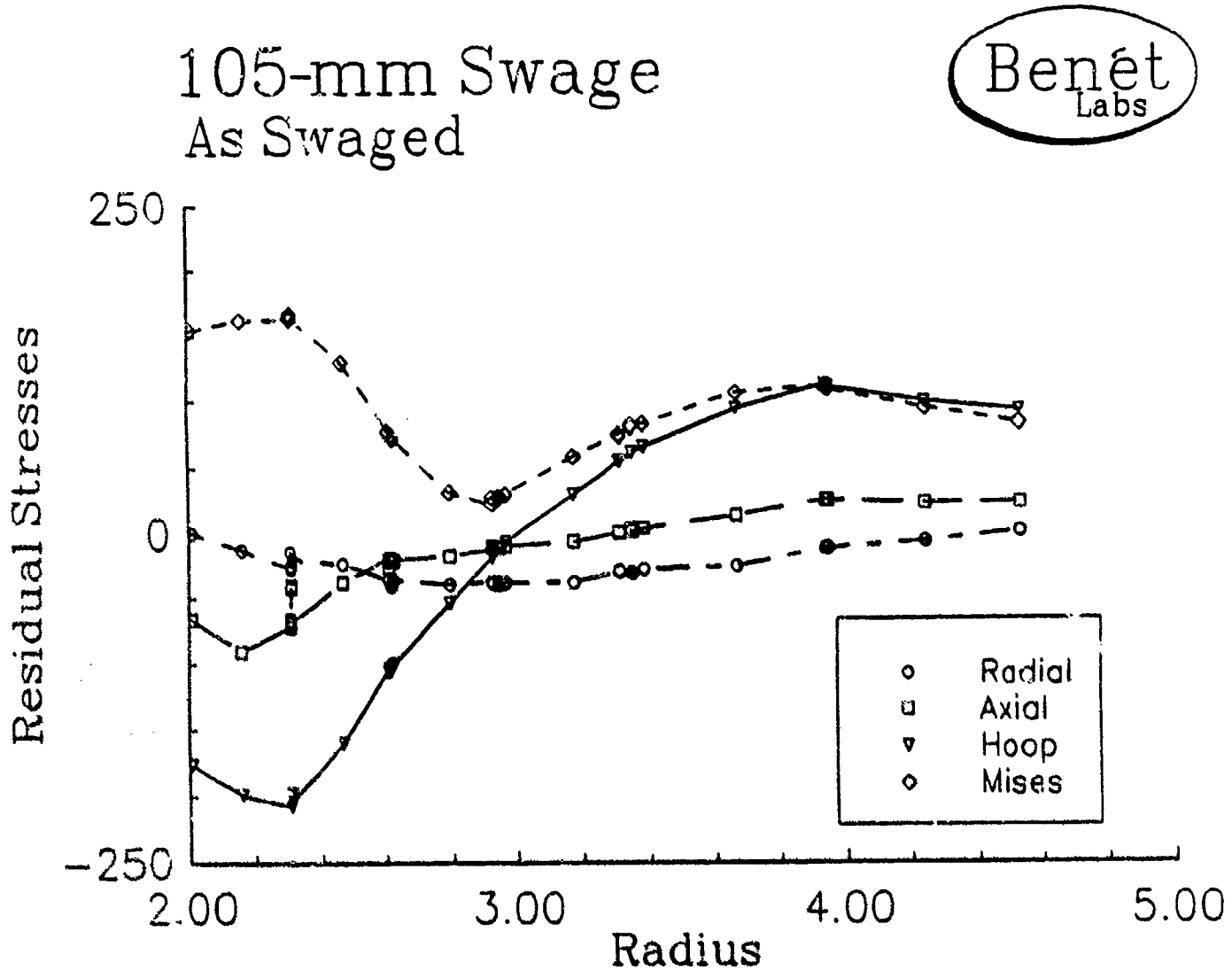

Figure 14. ABAQUS predictions of residual stresses of a 105-mm symmetric cylinder using an alternative finite element method.

TECHNICAL REPORT INTERNAL DISTRIBUTION LIST

	NO. OF COPIES
CHIEF, DEVELOPMENT ENGINEERING DIVISION	
ATTN: SMCAR-CCB-DA	1
-DC	1
-DI	1
-DR	1
-DS (SYSTEMS)	1
CHIEF, ENGINEERING SUPPORT DIVISION	
ATTN: SMCAR-CCB-S	1
-SD	1
-SE	1
CHIEF, RESEARCH DIVISION	
ATTN: SMCAR-CCB-R	2
-RA	1
-RE	1
-RM	1
-RP	1
-RT	1
TECHNICAL LIBRARY	5
ATTN: SMCAR-CCB-TL	
TECHNICAL PUBLICATIONS & EDITING SECTION	3
ATTN: SMCAR-CCB-TL	
OPERATIONS DIRECTORATE	1
ATTN: SMCWV-ODP-P	
DIRECTOR, PROCUREMENT DIRECTORATE	1
ATTN: SMCWV-PP	
DIRECTOR, PRODUCT ASSURANCE DIRECTORATE	1
ATTN: SMCWV-QA	

NOTE: PLEASE NOTIFY DIRECTOR, BENET LABORATORIES, ATTN: SMCAR-CCB-TL, OF ANY ADDRESS CHANGES.

TECHNICAL REPORT EXTERNAL DISTRIBUTION LIST

	NO. OF COPIES
ASST SEC OF THE ARMY RESEARCH AND DEVELOPMENT ATTN: DEPT FOR SCI AND TECH THE PENTAGON WASHINGTON, D.C. 20310-0103	1
ADMINISTRATOR DEFENSE TECHNICAL INFO CENTER ATTN: DTIC-FDAC CAMERON STATION ALEXANDRIA, VA 22304-6145	12
COMMANDER US ARMY ARDEC	
ATTN: SMCAR-AEE	1
SMCAR-AES, BLDG. 321	1
SMCAR-AET-O, BLDG. 351N	1
SMCAR-CC	1
SMCAR-CCP-A	1
SMCAR-FSA	1
SMCAR-FSM-E	1
SMCAR-FSS-D, BLDG. 94	1
SMCAR-IMI-I (STINFO) BLDG. 59	2
PICATINNY ARSENAL, NJ 07806-5000	
DIRECTOR US ARMY BALLISTIC RESEARCH LABORATORY ATTN: SLCBR-DD-T, BLDG. 305 ABERDEEN PROVING GROUND, MD 21005-5066	1
DIRECTOR US ARMY MATERIEL SYSTEMS ANALYSIS ACTV ATTN: AMXSY-MP ABERDEEN PROVING GROUND, MD 21005-5071	1
COMMANDER HQ, AMCCOM ATTN: AMSMC-IMP-L ROCK ISLAND, IL 61299-6000	1
COMMANDER ROCK ISLAND ARSENAL ATTN: SMCRI-ENM ROCK ISLAND, IL 61299-5000	1
DIRECTOR US ARMY INDUSTRIAL BASE ENGR ACTV ATTN: AMXIB-P ROCK ISLAND, IL 61299-7260	1
COMMANDER US ARMY TANK-AUTMV R&D COMMAND ATTN: AMSTA-DDL (TECH LIB) WARREN, MI 48397-5000	1
COMMANDER US MILITARY ACADEMY ATTN: DEPARTMENT OF MECHANICS WEST POINT, NY 10996-1792	1
US ARMY MISSILE COMMAND REDSTONE SCIENTIFIC INFO CTR ATTN: DOCUMENTS SECT, BLDG. 4484 REDSTONE ARSENAL, AL 35898-5241	2
COMMANDER US ARMY FGN SCIENCE AND TECH CTR ATTN: DRXST-SD 220 7TH STREET, N.E. CHARLOTTESVILLE, VA 22901	1
COMMANDER US ARMY LABCOM MATERIALS TECHNOLOGY LAB ATTN: SLCMT-IML (TECH LIB) WATERTOWN, MA 02172-0001	2

NOTE: PLEASE NOTIFY COMMANDER, ARMAMENT RESEARCH, DEVELOPMENT, AND ENGINEERING CENTER, US ARMY AMCCOM, ATTN: BENET LABORATORIES, SMCAR-CCB-TL, WATERVLIET, NY 12189-4050, OF ANY ADDRESS CHANGES.

TECHNICAL REPORT EXTERNAL DISTRIBUTION LIST (CONT'D)

	NO. OF COPIES
COMMANDER US ARMY LABCOM, ISA ATTN: SLCIS-IM-TL 2800 POWDER MILL ROAD ADELPHI, MD 20783-1145	1
COMMANDER US ARMY RESEARCH OFFICE ATTN: CHIEF, IPO P.O. BOX 12211 RESEARCH TRIANGLE PARK, NC 27709-2211	1
DIRECTOR US NAVAL RESEARCH LAB ATTN: MATERIALS SCI & TECH DIVISION CODE 26-27 (DOC LIB) WASHINGTON, D.C. 20375	1 1
DIRECTOR US ARMY BALLISTIC RESEARCH LABORATORY ATTN: SLCBR-IB-M (DR. BRUCE BURNS) ABERDEEN PROVING GROUND, MD 21005-5066	1
COMMANDER AIR FORCE ARMAMENT LABORATORY ATTN: AFATL/MN EGLIN AFB, FL 32542-5434	1
COMMANDER AIR FORCE ARMAMENT LABORATORY ATTN: AFATL/MNF EGLIN AFB, FL 32542-5434	1
MIAC/CINDAS PURDUE UNIVERSITY 2595 YEAGER ROAD WEST LAFAYETTE, IN 47905	1

NOTE: PLEASE NOTIFY COMMANDER, ARMAMENT RESEARCH, DEVELOPMENT, AND ENGINEERING CENTER, US ARMY AMCCOM, ATTN: BENET LABORATORIES. SMCAR-CCB-TL, WATERVLIET, NY 12189-4050, OF ANY ADDRESS CHANGES.